PERGAMON

Journal of Structural Geology 21 (1999) 1525–1534

JOURNAL OF STRUCTURAL GEOLOGY

www.elsevier.nl/locate/jstrugeo

Delineation of deformation grades of low-strain granitoids using assemblages of elementary deformation textures

Kazuo Kosaka[a,*], Masaaki Shimizu[b], Shigeru Takizawa[c]

[a]*Department of Geosystem Sciences, Nihon University, Setagaya, Tokyo 156-8550, Japan*
[b]*Department of Earth Sciences, Toyama University, Toyama 930-8555, Japan*
[c]*Institute of Geoscience, University of Tsukuba, Tsukuba, Ibaraki 305-8575, Japan*

Received 16 October 1998; accepted 20 May 1999

Abstract

Based on microscopic observations of the Miocene Tokuwa granodiorite, central Japan, a method of delineating deformation grades of low-strain granitoids has been derived which utilizes assemblages of elementary deformation textures (EDTs) such as subdomains in quartz, bent twins in plagioclase and kink-bands in biotite. Although the granodiorite is comprised of equant grains and shows no evidence of deformation to the naked eye except for brittle fractures, it shows a variety of EDTs at the microscale. In thin section, assemblages of EDTs belonging to quartz, plagioclase or biotite are used for deformation grading of the corresponding rock. The deformation grading by EDTs based on quartz correlates with deformation grading based on plagioclase or biotite. *Eigenvalues* derived from a principal component analysis indicate that the first principal component explains approximately three-quarters of the variance of deformation grading by EDTs based on quartz, plagioclase, and biotite. The deformation grading by EDTs using quartz correlates well with the first principal component score. These results indicate that the deformation grading by assemblages of EDTs based on quartz, as well as on the first principal component score, is useful for deformation grading of low-strain granitoids.

1. Introduction

Structural geology has been focused to some extent on strongly deformed minerals and rocks, and little attention has been paid to homogeneous and isotropic undeformed-looking granitoids. These latter rocks contain many important and interesting features inherited from the original rocks before deformation and due to incipient deformation. The calibration of intensities or grades of deformation in low-strain granitoids, known as deformation zoning, is a difficult task. This paper describes a method of deformation grading of low-strain granitoids using assemblages of elementary deformation textures (abbreviated as EDTs hereafter) such as subdomains in quartz, bent twins in plagioclase, and kink-bands in biotite. The presented method can be used for delineating the deformation grading and deformation condition of homogeneous and isotropic undeformed-looking granitoids.

EDTs have been previously used to describe strain in rocks, e.g. by Balk (1952) and Higgins (1971). Individual EDTs have been intensely studied in quartz (e.g. deformation lamellae, Carter et al., 1964; porphyroclasts, Bouchez, 1977; fine grains in mylonite, Lister and Price, 1978; ribbons, Vauchez, 1980), in feldspars (e.g. porphyroclasts, Debat et al., 1975, 1978; undulose extinction, deformation twins and new grains, Olsen and Kohlstedt, 1985; fractured feldspars in mylonite, Michibayashi, 1996), and in biotite (e.g. kink-bands and bent cleavages, Wilson and Bell, 1979; mica fish, Eisbacher, 1970; Lister and Snoke, 1984). However, the systematic use or statistical treatment of EDTs is restricted to a few papers dealing with naturally or experimentally deformed granitoids (e.g. Krupicka and Sassano, 1972; Wilson, 1973; Bell and Etheridge, 1976; Tullis and Yund, 1977; Kosaka, 1980;

* Corresponding author.
E-mail address: kosaka@chs.nihon-u.ac.jp (K. Kosaka)

0191-8141/99/$ - see front matter
PII: S0191-8141(99)00112-1

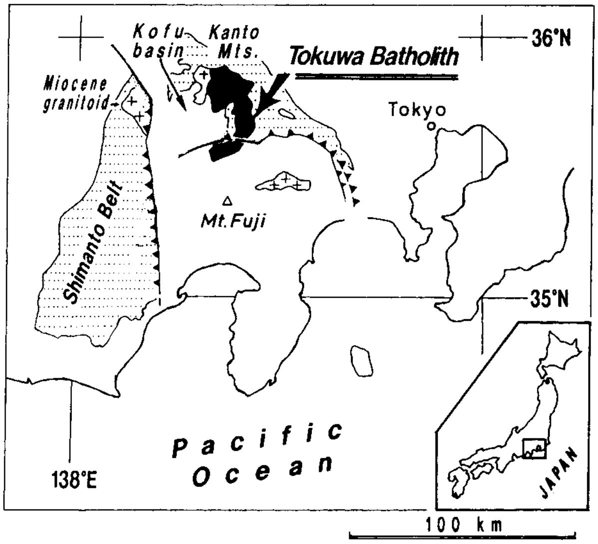

Fig. 1. Map showing the location of the Tokuwa batholith.

Takagi, 1984; Pryer, 1993). Since different deformation processes occur in different minerals at various stages of the deformation history (e.g. Burg and Laurent, 1978; Bossière and Vauchez, 1978; Wilson and Bell, 1979; Wenk and Pannetier, 1990), combinations of EDTs belonging to different minerals could provide much information on deformation processes. For example, a combination of recrystallized feldspars and recrystallized quartz in a mylonite indicates deformation at a higher temperature and/or lower differential stress than a texture combining fractured feldspars and recrystallized quartz (e.g. Kosaka, 1980). Similarly, the combination of deformation lamellae and deformation twins in plagioclase indicates a higher temperature and confining pressure than a combination of deformation lamellae and intragranular microcracks (Seifert and VerPloeg, 1977). In this paper, assemblages of EDTs are used for grading deformation textures in thin sections of the Tokuwa granodiorite in central Japan. For this purpose, samples were taken from the whole area, and more than 150 thin sections were examined under the microscope. Statistical analysis of 24 kinds of EDTs belonging to quartz, plagioclase, and biotite reveals that assemblages of EDTs provide a reliable basis for deformation grading of low-strain granitoids, even though optical microstructures alone are not always a reliable guide to dislocation structures (Tullis and Yund, 1977).

2. Geological setting

The Tokuwa batholith is situated at the southwestern corner of the Kanto Mountains to the east of the Kofu basin, near Tokyo and Mount Fuji in central Japan (Fig. 1). It is 42 km long in its north–south direction and 26 km wide east–west in maximum, and it covers an area of about 300 km^2. It intruded the Shimanto belt, an accretion zone of Cretaceous/Paleogene strata (Ogawa and Horiuchi, 1978), during the late Middle Miocene (Mimura et al., 1984). It has been dated by several methods: 9.3 Ma (Rb–Sr, whole rock: ECGMYP, 1970), 10.2–13.0 Ma (K–Ar ages of biotite: Kawano and Ueda, 1964, 1966; Shibata et al., 1984), and 10–12 Ma (FT ages of zircon: Nishiyama, 1989). The Tokuwa batholith is composed mainly of medium-grained granodiorites with some gabbros and diorites at the center and some hornblende–biotite granodiorites to granites at the periphery (Shimizu, 1986). It is composed of both ilmenite- and magnetite-series granitoids, based on the criteria of Ishihara (1977). These granitoids are composed mainly of quartz, orthoclase, plagioclase, biotite, and amphibole (Shimizu, 1986). They are composed of equant grains and show no macroscopic evidence of deformation except for joints and brittle faults. They contain microgranitoid enclaves in places, but no deformation is visible in the field. However, the Tokuwa batholith shows various EDTs under the microscope (Fig. 2a) in the 162 thin sections of granodiorite which has been sampled at 162 different localities, covering the whole area and ranging in altitude from 580 to 1900 m.

Bedding in the sediments surrounding the Tokuwa batholith is subvertical and tightly folded, mostly trending northwest to west-southwest (Ogawa and Horiuchi, 1978; Sakai, 1987). The overall strike and dip of these strata do not vary around the batholith, and this, along with other evidence such as abundant xenoliths of country rocks, suggests that the intrusion occurred by magmatic stoping rather than by diapirism or forcible emplacement (Shimizu, 1986). The undisturbed country rocks also suggest little post-emplacement deformation, which would tend to accumulate strain at the batholith margin.

3. Deformation grading

3.1. Deformation grading of individual minerals

Seven EDTs are listed for quartz (Table 1a): the first

Fig. 2. Photomicrographs of deformation textures in the Tokuwa batholith. (a) An example of a highly deformed texture. The deformation grade of quartz is IIIa. (b) Simple undulose extinction in quartz (large grain in the center). (c) Jigsaw-puzzle undulose extinction in quartz (in most of the picture). Notice microcracks which are overprinted on the EDTs. (d) Banded undulose extinction in quartz. (Arrows indicate band boundaries.) (e) Large subdomains in quartz. (Isolated subdomains are indicated by arrows.) (f) Subdomain twig in quartz (arrows). (g) Subdomain cluster, i.e. a cluster of large subdomains in quartz (in most of the picture). (h) Small subdomain in quartz (arrow). (i) Simple undulose extinction in plagioclase (in the large central grain). (j) Jigsaw-puzzle undulose extinction in plagioclase (in most of the picture).

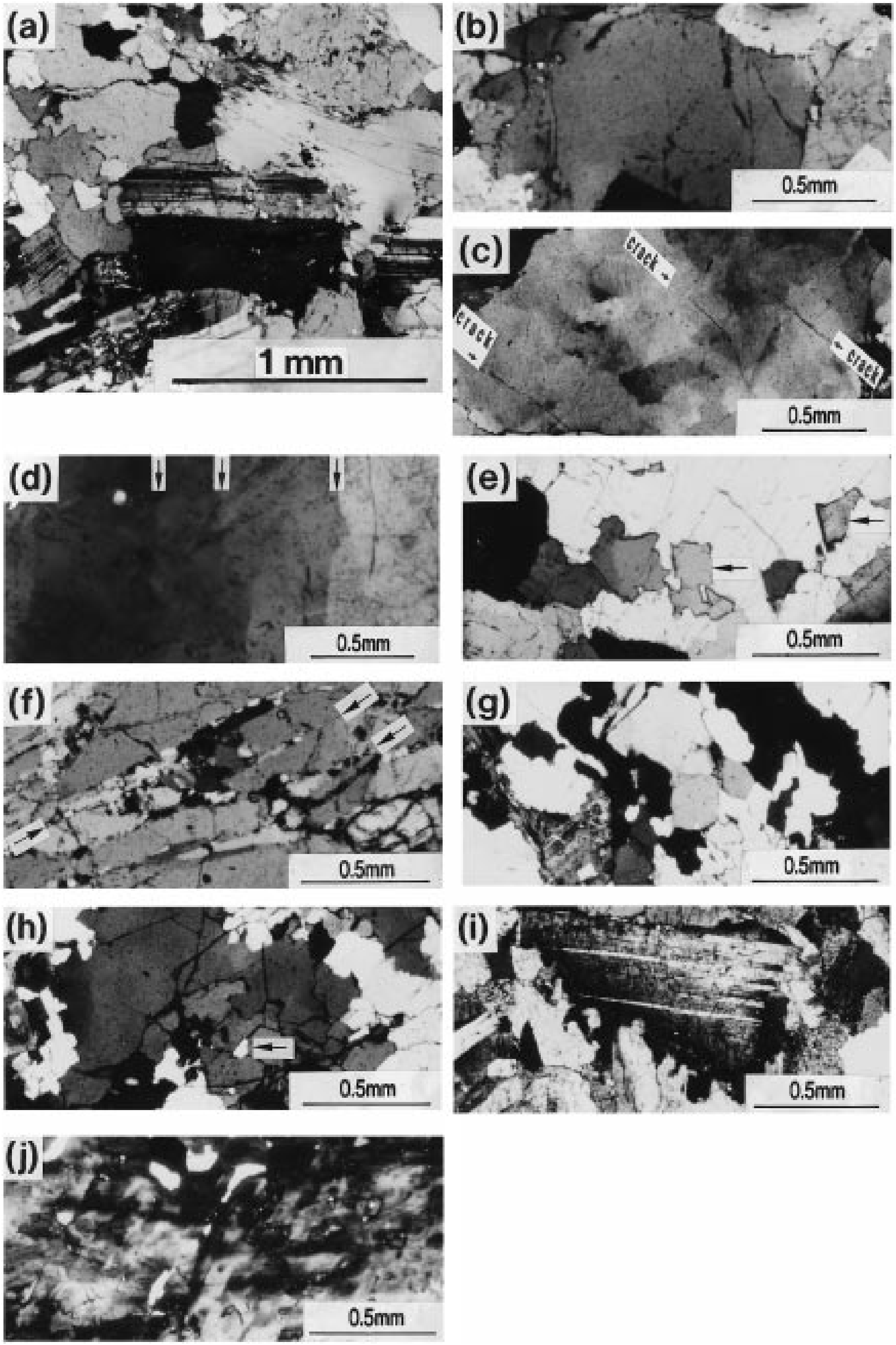
(a)
1 mm
(b)
0.5mm
(c)
crack
crack
crack
0.5mm
(d)
0.5mm
(e)
0.5mm
(f)
0.5mm
(g)
0.5mm
(h)
0.5mm
(i)
0.5mm
(j)
0.5mm

Table 1
Explanation of elementary deformation textures (EDTs) of quartz, plagioclase and biotite

(a) Elementary deformation textures (EDTs) of quartz			
Simple undulose extinction	A slight, gradational variation in the extinction angle within a grain.	Fig. 2	b
Jigsaw-puzzle undulose extinction	An extinction showing a pattern of jigsaw-puzzle chips.		c
Banded undulose extinction	An extinction sweeping from band to band throughout a grain.		d
Large subdomain	An isolated subdomain of more than 100 μm in size, including the case of a subgrain in the sense that it is separated from the host by sharp boundaries, and shows a quite different extinction with respect to the host through planar boundaries (e.g. Hobbs et al., 1976; p. 96).		e
Subdomain twig	A set of cracks or healed cracks and subdomains that are tens of microns in size, arranged like leaves along a branch.		f
Subdomain cluster	A cluster of subdomains, or subgrains, up to hundreds of microns in size, within which very slight differences in extinction appear from one subdomain to the other.		g
Small subdomain	A small subdomain, tens of microns in size, possibly a new grain, as shown by its high-angle boundaries and quite different extinction orientation from neighbouring quartz (see Hobbs et al., 1976; p. 96).		h
(b) Elementary deformation textures (EDTs) of plagioclase			
Simple undulose extinction	A slight, gradational variation in the extinction angle within a grain.	Fig. 2	i
Jigsaw-puzzle undulose extinction	An extinction showing a pattern of jigsaw-puzzle chips.		j
Banded undulose extinction	An extinction sweeping from band to band throughout a grain.	Fig. 3	a
Bent twins	Curviplanar twin surfaces.		b
Intragranular microfault	An intragranular microfault cutting and displacing twins.		b
Slipped twin/slipped cleavage	An offset along microfaults on twin or cleavage surface.		c
Kink band	Kink band in the usual sense.		d
Mechanical twins	Mechanical twins in the usual sense, consisting of smaller-sized and wedge-shaped twins on grain margins (e.g. Nicolas, 1987).		e
(c) Elementary deformation textures (EDTs) of biotite			
Undulose extinction	Undulose extinction in the usual sense.	Fig. 3	f
Bent cleavages	Curviplanar cleavages.		f
Kink band	Kink band in the usual sense.		g
Cusped cleavages	An intragranular cuspate microfold.		h
Pseudostylolite	A textural feature similar to stylolite in limestone.		i
En échelon microfolds	En échelon microfolds which appear like wrinkles.		j
Split cleavage	A quartz lamella along a cleavage plane in biotite.		k
Intragranular microfault	Cutting and displacing cleavages, or occurring on a cleavage surface; the latter case may also be classified as a slipped cleavage.		–
Fine biotite grain	A recrystallized fine biotite grain into a strained host grain of biotite.		l

three are concerned with undulose extinction (Fig. 2b–d), and the other four with subdomains (Fig. 2e–h). Among them, some small subdomains include irregular basal (or near-basal) subgrain boundaries. In plagioclase, eight EDTs have been recognized (Table 1b): the first three are concerned with undulose extinction (Figs. 2i, j and 3a), the next four with microfolding or microfaulting (Fig. 3b–d), and the last with twinning (Fig. 3e). In biotite, nine EDTs have been recognized (Table 1c): they are concerned with microfolding or microfaulting except for the last EDT (Fig. 3f–l), which concerns fine recrystallized biotite grains. In orthoclase and amphibole, no EDTs other than undulose extinctions and intragranular microcracks occur.

Each thin section has been assigned to a particular deformation grade, according to its assemblage of EDTs belonging to quartz, plagioclase, and biotite. For quartz, seven grades, from Ia to IIIb, have been distinguished. The corresponding assemblages are shown in Fig. 4(a) and their areal distribution in the batholith is plotted in Fig. 5. Grades I, II, and III correspond to undulose extinctions alone, discrete subdomains, and subdomain clusters, respectively. Within grade I, grade Ia corresponds to simple undulose

Fig. 3. Photomicrographs of deformation textures in the Tokuwa batholith (continued). (a) Banded undulose extinction in plagioclase (arrow). Notice a microcrack which is overprinted on the EDT. (b) Bent twins (left arrow) and intragranular microfault (right arrow) in plagioclase. (c) Slipped twin in plagioclase (arrows). (d) Kink-band in plagioclase (arrows). (e) Mechanical twins in plagioclase (arrow). (f) Undulose extinction (whole area) and bent cleavages (left) in biotite. (g) Kink-bands in biotite. (h) Cusped cleavages in biotite (arrows). (i) Pseudostylolite in biotite (arrows). (j) En échelon microfolds in biotite (arrows). (k) Split cleavages in biotite (arrows). (l) Fine biotite grains in a strained host grain of biotite (arrows).

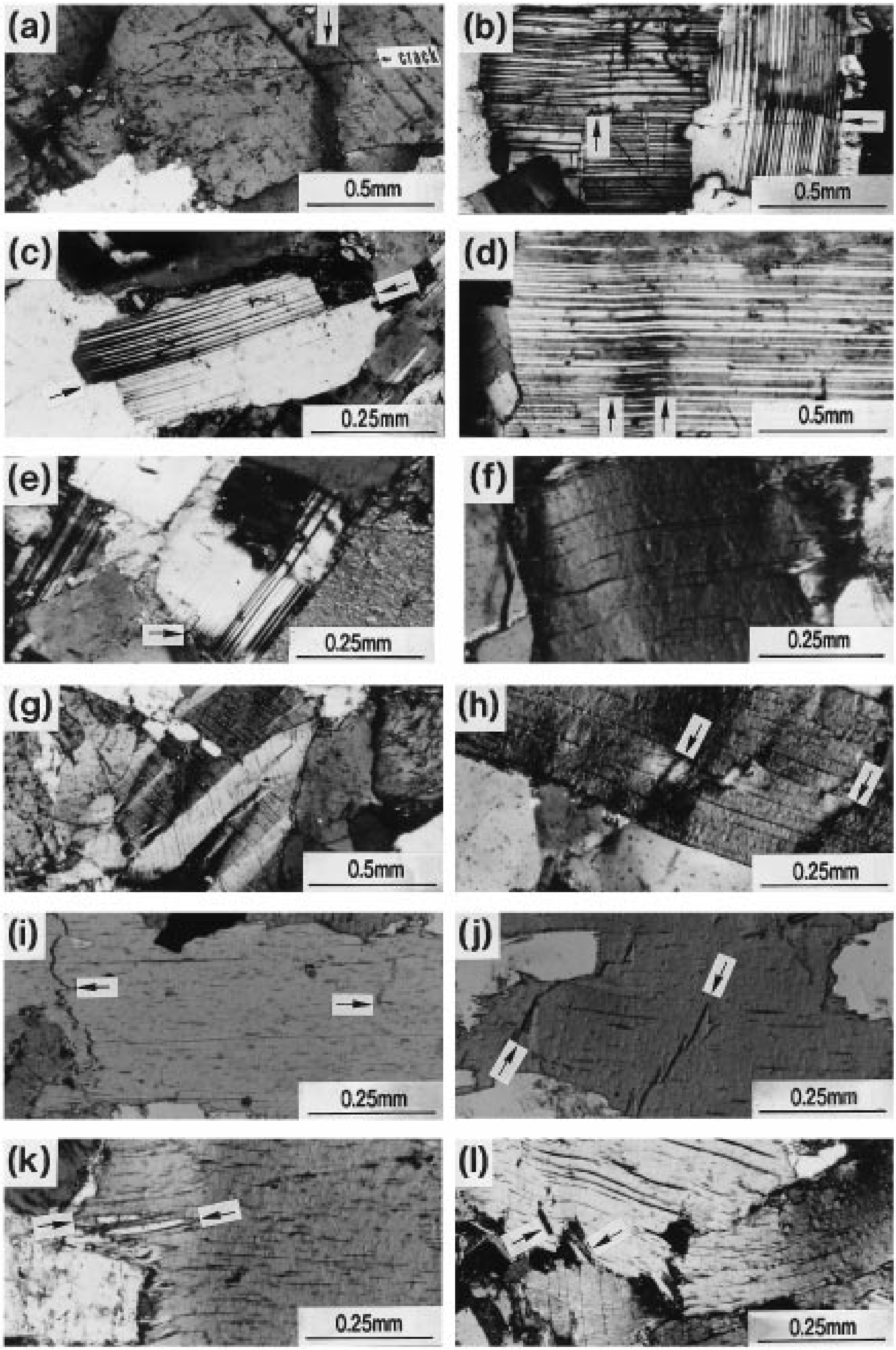
(a)
crack
0.5mm
(b)
0.5mm
(c)
0.25mm
(d)
0.5mm
(e)
0.25mm
(f)
0.25mm
(g)
0.5mm
(h)
0.25mm
(i)
0.25mm
(j)
0.25mm
(k)
0.25mm
(l)
0.25mm

(a) Quartz

Elementary Deformation Textures (EDTs)	Deformation grades I a	I b	I c	II a	II b	III a	III b
Simple undulose extinction	====	====	====	====	====	====	====
Jigsaw-puzzle undulose extinction		-----=	--=--=	====	====	====	====
Banded undulose extinction			-----=	--=--=	--=--=	====	====
Large subdomain (s)				-----=	====	====	====
Subdomain twig (s)					------		
Subdomain cluster (s)						------	------
Small subdomain (s)							------
Intragranular microcrack (s)	====	====	====	====	====	====	====
Intragranular healed microcrack (s)	--=--=	--=--=	--=--=	--=--=	--=--=	--=--=	-=--=

(b) Plagioclase

Elementary Deformation Textures (EDTs)	Deformation grades 0	1	2	3	4	5
Simple undulose extinction		-----= ====	====	====	====	====
Jigsaw-puzzle undulose extinction Banded undulose extinction			------ ------	------ ------	------ ------	------ ------
Bent twins		•		------	------	------
Intragranular microfault (s)		•	•		------	------
Slipped twin (s)/Slipped cleavage (s) Kink band (s) Mechanical twins				•		------
Intragranular microcrack (s)	------	------ ------	------	------	------	------

(c) Biotite

Elementary Deformation Textures (EDTs)	Deformation grades 1	2	3	4	5	6	7
Undulose extinction	====	====	====	====	====	====	====
Bent cleavages		------	----==	====	====	====	====
Kink band (s)			------	------	----==	====	====
Cusped cleavages	•			------	------	------	------
Pseudostylolite (s)	•	•	•		- ----	------	------
En echelon microfolds	•	•	•		-----	------	------
Split cleavage (s)			•	•		------	------
Intragranular microfault (s)						------	------
Fine biotite grain (s)							------
Intragranular microcrack (s)	------	------	------	------	------	------	------

[ ] None [•] Exceptional [------] Rare to few [-=-=] Few to common [====] Common to almost all

Fig. 4. Deformation grading of granitoid by assemblages of elementary deformation textures (EDTs) of quartz (a), plagioclase (b) and biotite (c). 'Exceptional' means that the corresponding EDT is found only in one or two exceptional thin section(s). 'Rare to few', 'Few to common' and 'Common to almost all' relate to the occurrence of corresponding EDT in thin sections of the corresponding grade.

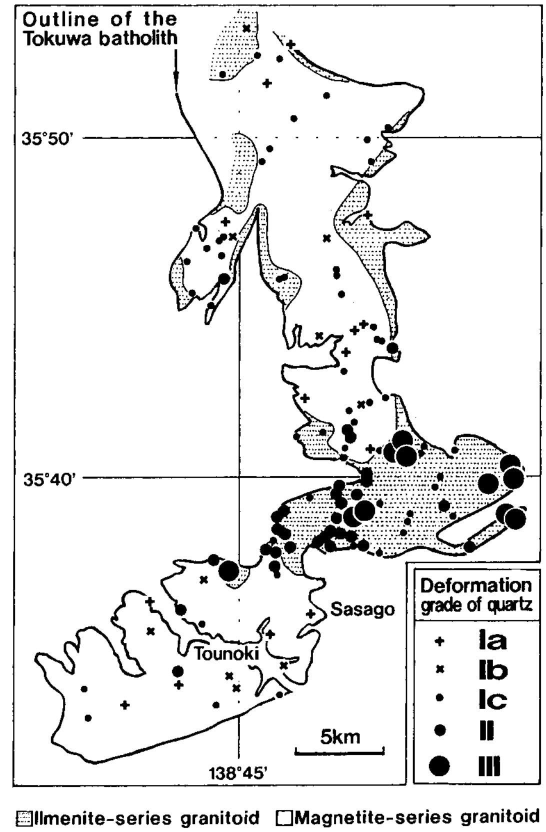

Fig. 5. Areal distribution of deformation grades of quartz in the Tokuwa batholith.

extinction alone; grade Ib corresponds to the assemblage of simple and jigsaw-puzzle undulose extinctions; grade Ic corresponds to the assemblage of simple, jigsaw-puzzle and banded undulose extinctions. Note that all the 162 thin sections have been arranged in Fig. 4(a) with respect to the listed EDTs without apparent contradiction through trial and error. In other words, any given thin section is classified into just one of these seven grades (Ia–IIIb), though 'a' and 'b' of grades II and III are not shown in Fig. 5 and later figures due to the small number of thin sections. In Fig. 5, deformation grading of quartz in magnetite-series granitoids does not exceed grade I, while in ilmenite-series granitoids it ranges from Ic to III. Based on our available data, there are no gradual changes in deformation grading of quartz over the whole area either laterally or from lower to higher altitudes. For plagioclase and biotite, deformation grading can be performed just as for quartz, although some exceptional thin sections may occur (Figs. 4b, c); for example, some thin sections are assigned to the grade 1, in the case of plagioclase, because of a lack of 'jigsaw-puzzle' and 'banded undulose extinctions', and yet they contain 'bent twins' or 'intragranular microfault(s)'. Healed microcracks in quartz and non-healed microcracks in all the minerals occur in every thin section, and commonly overprint the whole microstructure as shown in the micrographs of Figs. 2(c) and 3(a) and noted in Fig. 4(a)–(c). Carefully prepared thin sections show that the microcracks formed under a regional stress field after the formation of EDTs (Kosaka et al., 1999). Therefore, they were not included in the deformation grading.

3.2. Deformation grading of whole thin sections

Since the density deformation features in quartz, plagioclase, and biotite vary greatly, the overall rock deformation is commonly graded by the principal components of deformation grades of these minerals. In order to obtain a ranking of the overall rock deformation, the following grades are introduced:

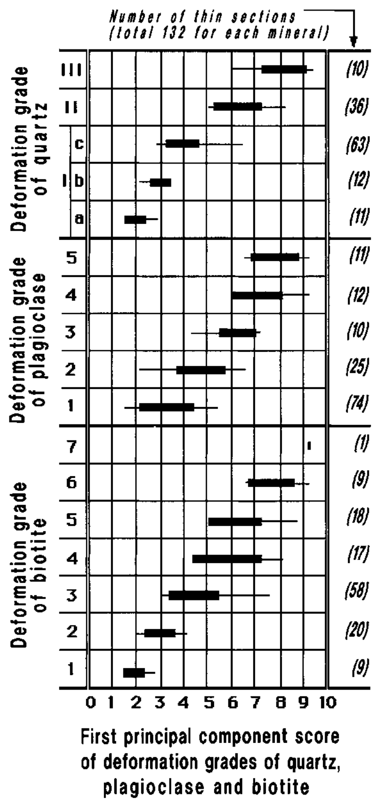

Fig. 6. Correlation between the first principal component score of deformation grades (abscissa) and the deformation grades of quartz, plagioclase and biotite (ordinals). Wide-bar: mean ± one sample standard deviation, narrow-bar: range from minimum to maximum.

Qtz = a scale from 1 to 7; 1 (for Ia), 2 (for Ib), ... ,
and 7 (for IIIb):

Pl = a scale from 1 to 5;

Bt = a scale from 1 to 7.

Then, using the method of multivariate statistical analysis of Kendall (1975), the three principal components of deformation are derived:

First principal component:

$0.55 \times \text{Qtz} + 0.52 \times \text{Pl} + 0.56 \times \text{Bt}$ (*eigenvalue* 464);

Second principal component:

$-0.17 \times \text{Qtz} - 0.58 \times \text{Pl} + 0.80 \times \text{Bt}$ (*eigenvalue* 121);

Third principal component:

$0.82 \times \text{Qtz} - 0.54 \times \text{Pl} - 0.21 \times \text{Bt}$ (*eigenvalue* 58).

The coefficient numbers given here, (0.55, 0.52, 0.56), (−0.17, − 0.58, 0.80), and (0.82, − 0.54, − 0.21), are *eigenvectors* corresponding to the cited *eigenvalues* 464, 121, and 58, respectively. The first principal component has a large *eigenvalue*, which accounts for about three-quarters of the variance in deformation grades of the three given minerals $[= 72\% = 464/(464 + 121 + 58)]$. For example, if in a given thin section the grades are Ic for quartz, 1 for plagioclase, and 3 for biotite, then the principal component scores are: first score $= 0.55 \times 3 + 0.52 \times 1 + 0.56 \times 3 = 3.85$; second score $= -0.17 \times 3 - 0.58 \times 1 + 0.80 \times 3 = 1.31$; and third score $= 0.82 \times 3 - 0.54 \times 1 - 0.21 \times 3 = 1.29$.

Fig. 6 illustrates the positive correlations observed between values of the first principal component score and the deformation grades of quartz, plagioclase and biotite. The deformation grading of quartz correlates best with the first principal component score, but the deformation gradings of plagioclase and biotite also display a good correlation. However, the deformation gradings of plagioclase and biotite do not correlate well with each other (Fig. 7c). Therefore, the deformation grading of quartz may replace the first principal component to represent the overall deformation intensity to best advantage.

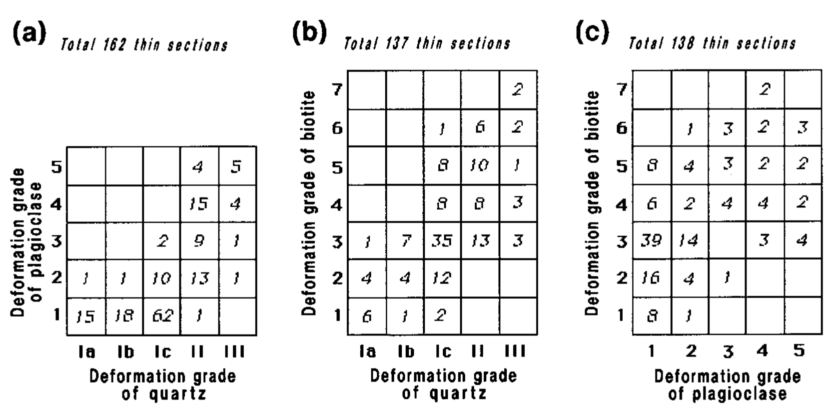

(a) Quartz vs plagioclase (Total 162 thin sections)

Plagioclase grade	Ia	Ib	Ic	II	III
5				4	5
4				15	4
3			2	9	1
2	1	1	10	13	1
1	15	18	62	1	

(b) Quartz vs biotite (Total 137 thin sections)

Biotite grade	Ia	Ib	Ic	II	III
7					2
6			1	6	2
5			8	10	1
4			8	8	3
3	1	7	35	13	3
2	4	4	12		
1	6	1	2		

(c) Plagioclase vs biotite (Total 138 thin sections)

Biotite grade	1	2	3	4	5
7				2	
6		1	3	2	3
5	8	4	3	2	2
4	6	2	4	4	2
3	39	14		3	4
2	16	4	1		
1	8	1			

Fig. 7. Contingency tables among deformation grades of quartz, plagioclase and biotite. (a) Quartz vs plagioclase. (b) Quartz vs biotite. (c) Plagioclase vs biotite. *Italics* represent numbers of thin sections.

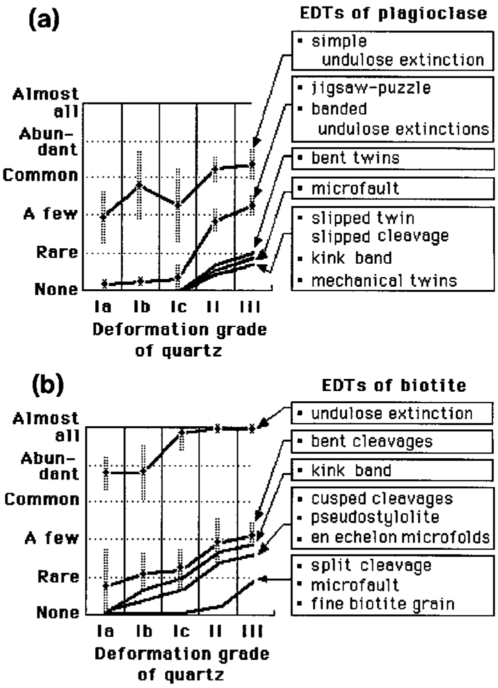

Fig. 8. Quantities of elementary deformation textures (EDTs) of plagioclase (a) and biotite (b) vs deformation grade of quartz. Vertical bars of upper two lines in (a) and (b) indicate one standard deviation.

Fig. 8 represents the abundance of EDTs of plagioclase and biotite vs the increasing deformation grade of quartz. In grade Ia, a few plagioclase grains have simple undulose extinctions and no other EDTs are observed (Fig. 8a), while many biotite grains already have undulose extinctions, and few biotite grains have bent cleavage planes (Fig. 8b). With increasing deformation of quartz, the EDTs of plagioclase and biotite also increase generally. In grade III, every type of EDT occurs pervasively in plagioclase and biotite.

3.3. Deformation grading and petrographic features

Deformation grading enables us to correlate low-strain granitoids with their petrographic features (Fig. 9). Based on the available data (Shimizu, 1986), 60 thin sections are classified into three groups based on magnetic susceptibility. The deformation grades of the group of lower magnetic susceptibility are generally higher than those of higher magnetic susceptibility (Fig. 9a). This tendency is also expressed in terms of magnetite modal percentage. The lower the magnetite modal percentage, the higher the deformation grade (Fig. 9b). The deformation grading also positively correlates with modal percentages of biotite and quartz (Figs. 9c, d), while it shows a negative correlation with the plagioclase content (Fig. 9e). Orthoclase, amphibole, and pyroxene percentages show no apparent correlation with deformation grades (Figs. 9f, g). No apparent positive correlation of SiO_2 percentage with the deformation grade is observed, partly due to the relatively small number of available thin sections (Fig. 9h).

4. Discussion and conclusion

Most EDTs of the Tokuwa granodiorite are considered to have formed at the latest stage of magma consolidation (about 700°C, 140 MPa, 5 km depth), or just after the total consolidation, based on the mode of deformation of EDTs (Kosaka et al., 1999). Strain intensity responsible for the EDTs is probably only a few percent. This is based on examination of the maximum strain of biotite, which is the most deformable mineral grain in the granodiorite, and also on the fact that the quartz grains retain their original equant outlines (Fig. 2a). Thus, the solid-state strains would be much less than 10%, as also suggested for the Barre granite which shows no detectable grain flattening nor mica alignment (Schedl et al., 1986).

Deformation grading is a useful tool to analyze deformation in the Earth's crust (e.g. review by Higgins, 1971). Several criteria have been used for deformation grading in strongly deformed rocks, such as the intensity of foliation/cleavage development (Goodwin and Wenk, 1995), the shape and orientation of markers (Debat et al., 1975; Burg and Laurent, 1978; Guglielmo, 1993), the presence or abundance of deformation textures (Bossière and Vauchez, 1978), grain size reduction (Shimamoto et al., 1991), crystallographic preferred orientation (Hara et al., 1973), or some combination of these criteria (Krupicka and Sassano, 1972). These criteria are, however, not applicable in low-strain rocks which preserve their original textures with the outlines of constituent grains unchanged. This is why EDTs in the constituent minerals could be used in deformation grading of low-strain granitoids. Since the EDTs vary from one mineral to the other and change depending on deformation conditions and total strain (Tullis et al., 1973; Tullis and Yund, 1977; Kosaka, 1980; Pryer, 1993), it is reasonable to use associations of the EDTs to subdivide intensity or grade of whole-rock deformation. In the case of the Tokuwa batholith, the deformation grade of each thin section is well defined by the first principal component of deformation grades determined by the EDTs of quartz, plagioclase and biotite, or by the deformation grades of quartz alone (Fig. 4).

The deformation features of low-strain Tokuwa batholith can therefore be summarized as follows. The diversity in deformation grade of quartz does not change gradually over the whole area, but depends on whether the samples belong to the magnetite- or ilmenite-series granitoids. The deformation of granitoids with higher amounts of quartz and biotite is rather intense compared to those with lower contents. This is

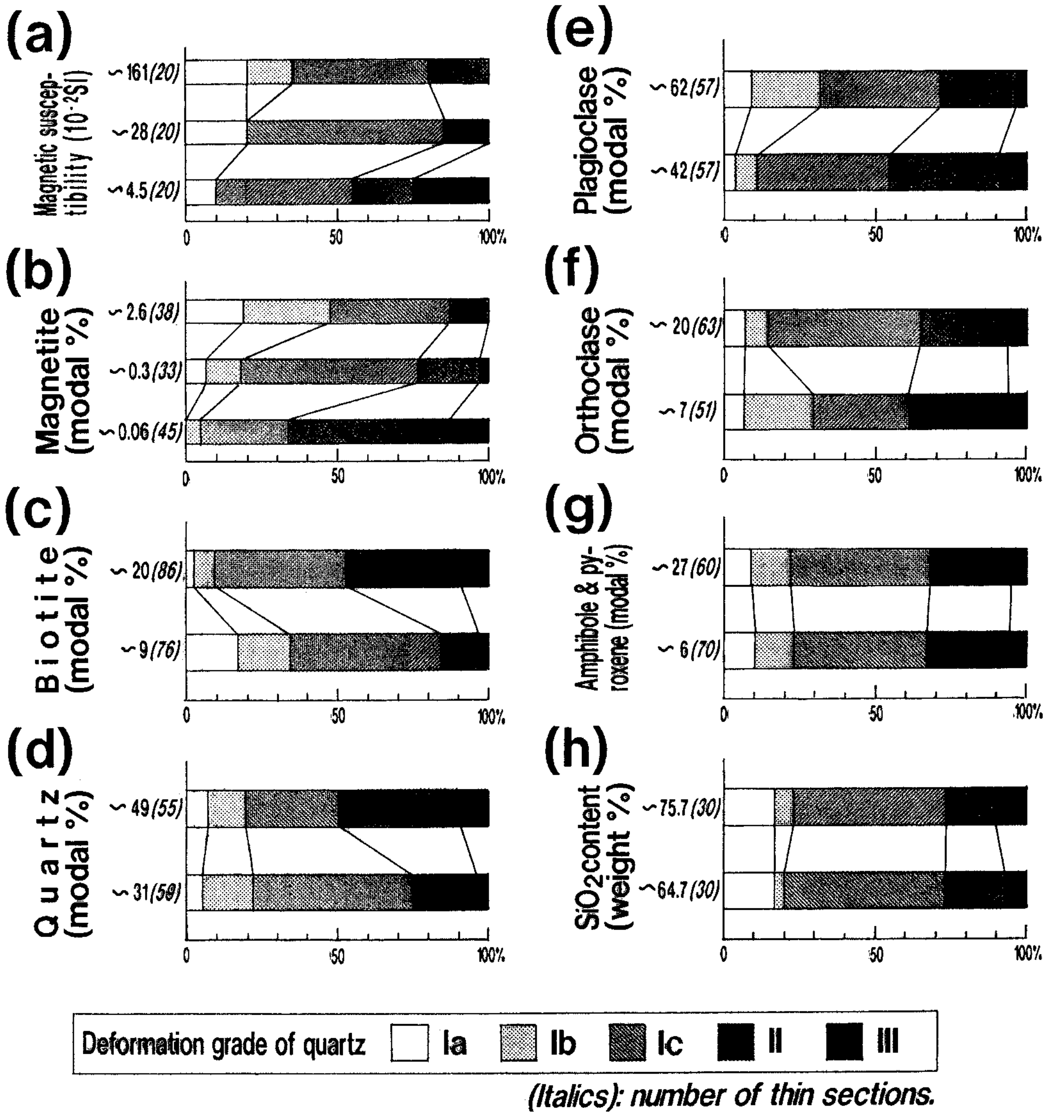

Fig. 9. Relations between quartz deformation intensity and other features. (a) Magnetic susceptibility. (b) Magnetite modal percentage. (c) Biotite modal percentage. (d) Quartz modal percentage. (e) Plagioclase modal percentage. (f) Orthoclase modal percentage. (g) Amphibole and pyroxene modal percentage. (h) SiO_2 content.

attributed to the fact that quartz- and mica-rich rocks are generally weaker than plagioclase-rich rocks at metamorphic conditions (e.g. Vernon and Flood, 1988; Kosaka et al., 1999). The influence of magnetite content is difficult to explain, but the presence of magnetite suggests a higher water content of the granitoid (Shimizu, 1986) and therefore could be associated with hydrolytic weakening of quartz (e.g. review by Paterson, 1989).

This study illustrates the potential usefulness of deformation grading of low-strain granitoids for the analysis of structures inherited from the original rocks before deformation, such as late magmatic deformation, and structures due to incipient deformation (Kosaka et al., 1999).

Acknowledgements

This study is partly funded by the Ministry of Education, Science, Sport and Culture of Japan (No. 07304044 to K.K. and M.S., No. 07640636 to M.S.) and by the Japan Mining Promotive Foundation (to M.S.).

References

Balk, R., 1952. Fabric of quartzites near thrust faults. Journal of Geology 60, 415–435.

Bell, T.H., Etheridge, M.A., 1976. The deformation and recrystallization of quartz in a mylonite zone, central Australia. Tectonophysics 32, 235–267.

Bossière, G., Vauchez, A., 1978. Déformation naturelle par cisaillement ductile d'un granite de Grande Kabylie occidentale (Algérie). Tectonophysics 51, 57–81.
Bouchez, J.L., 1977. Plastic deformation of quartzites at low temperature in an area of natural strain gradient. Tectonophysics 39, 25–50.
Burg, J.P., Laurent, P., 1978. Strain analysis of a shear zone in a granodiorite. Tectonophysics 47, 15–42.
Carter, N.L., Christie, J.M., Griggs, D.T., 1964. Experimental deformation and recrystallization of quartz. Journal of Geology 72, 687–733.
Debat, P., Sirieys, P., Deramond, J., Soula, J.C., 1975. Paléodéformations d'un massif orthogneissique (Massif des Cammazes, Montagne Noire occidentale, France). Tectonophysics 28, 159–183.
Debat, P., Soula, J.C., Kubin, L., Vidal, J.L., 1978. Optical studies of natural deformation microstructures in feldspars (gneiss and pegmatites from Occitania, southern France). Lithos 11, 133–145.
ECGMYP (Editorial Committee of Geologic Map of Yamanashi Prefecture) (Ed.), 1970. Geology of Yamanashi Prefecture, scale 1:100,000. Yamanashi Prefecture (in Japanese).
Eisbacher, G.H., 1970. Deformation mechanics of mylonitic rocks and fractured granites in Cobequid Mountains, Nova Scotia, Canada. Geological Society of America Bulletin 81, 2009–2020.
Goodwin, L.B., Wenk, H.R., 1995. Development of phyllonite from granodiorite: mechanisms of grain-size reduction in the Santa Rosa mylonite zone, California. Journal of Structural Geology 17, 689–707.
Guglielmo Jr., G., 1993. Magmatic strains and foliation triple points of the Merrimac plutons, northern Sierra Nevada, California: implications for pluton emplacement and timing of subduction. Journal of Structural Geology 15, 177–189.
Hara, I., Takeda, K., Kimura, T., 1973. Preferred lattice orientation of quartz in shear deformation. Journal of Science, Hiroshima University, Ser. C 7, 1–10.
Higgins, M.W., 1971. Cataclastic rocks. U.S. Geological Survey Professional Paper No. 687.
Hobbs, B.E., Means, W.D., Williams, P.F., 1976. An Outline of Structural Geology. John Wiley, New York.
Ishihara, S., 1977. The magnetite-series and ilmenite-series granitic rocks. Mining Geology 27, 293–305.
Kawano, Y., Ueda, Y., 1964. K–Ar dating on the igneous rocks in Japan (I). Journal of Japan Society of Petrology, Mineralogy and Mining Geology 51, 127–148 (in Japanese).
Kawano, Y., Ueda, Y., 1966. K–Ar dating on the igneous rocks in Japan (IV)—Granitic rocks in northeastern Japan. Journal of Japan Society of Petrology, Mineralogy and Mining Geology 56, 41–55 (in Japanese).
Kendall, M.G., 1975. Multivariate Analysis. Charles Griffin, London.
Kosaka, K., 1980. Fault-related fabrics of granitic rocks. Journal of the Faculty of Science, University of Tokyo, Sec. II 20, 77–115.
Kosaka, K., Shimizu, M., Takizawa, S., 1999. Late- to post-magmatic deformation of the Miocene Tokuwa granodiorite, central Japan. Resource Geology (in press).
Krupicka, J., Sassano, G.P., 1972. Multiple deformation of crystalline rocks in the Tazin group, Eldorado Fay Mine, NW Saskatchewan. Canadian Journal of Earth Science 9, 422–432.
Lister, G.S., Price, G.P., 1978. Fabric development in a quartz–feldspar mylonite. Tectonophysics 49, 37–78.
Lister, G.S., Snoke, A.W., 1984. *S–C* mylonites. Journal of Structural Geology 6, 617–638.
Michibayashi, K., 1996. The role of intragranular fracturing on grain size reduction in feldspar during mylonitization. Journal of Structural Geology 18, 17–25.
Mimura, K., Kato, Y., Katada, M., 1984. Geology of the Mitake–Shosenkyo district. Geological Survey of Japan (in Japanese with English abstract).
Nicolas, A., 1987. Principles of Rock Deformation. D. Reidel, Dordrecht.
Nishiyama, T., 1989. Fission-track ages of granitic rocks around Kofu Basin, central Japan. Abstract of 5th Workshop on ESR Applied Metrology (in Japanese).
Ogawa, Y., Horiuchi, K., 1978. Two types of accretionary fold belts in central Japan. Journal of Physics of the Earth 26 (Suppl.), 321–336.
Olsen, T.S., Kohlstedt, D.L., 1985. Natural deformation and recrystallization of some intermediate plagioclase feldspars. Tectonophysics 111, 107–131.
Paterson, M.S., 1989. The interaction of water with quartz and its influence in dislocation flow—an overview. In: Karato, S.-I., Toriumi, M. (Eds.), Rheology of Solids and of the Earth. Oxford University Press, Oxford, pp. 107–142.
Pryer, L.L., 1993. Microstructures in feldspars from a major crustal thrust zone: the Grenville Front, Ontario, Canada. Journal of Structural Geology 15, 21–36.
Sakai, A., 1987. Geology of the Itsukaichi district, with geological sheet map at 1:50,000. Geological Survey of Japan (in Japanese with English abstract).
Schedl, A., Kronenberg, A.K., Tullis, J., 1986. Deformation microstructures of Barre granite: an optical, SEM and TEM study. Tectonophysics 122, 149–164.
Seifert, K., VerPloeg, A.J., 1977. Deformational characteristics of experimentally deformed Adirondack anorthosite. Canadian Journal of Earth Science 14, 2706–2717.
Shibata, K., Kato, Y., Mimura, K., 1984. K–Ar ages of granites and related rocks from the northern Kofu area. Bulletin of Geological Survey of Japan 35, 19–24 (in Japanese).
Shimamoto, T., Kanaori, Y., Asai, K., 1991. Cathodoluminescence observations on low-temperature mylonites: potential for detection of solution–precipitation microstructures. Journal of Structural Geology 13, 967–973.
Shimizu, M., 1986. The Tokuwa batholith, central Japan: an example of occurrence of ilmenite-series and magnetite-series granitoids in a batholith. Bulletin of the University Museum, the University of Tokyo No. 28.
Takagi, H., 1984. Mylonitic rocks along the Median Tectonic Line in Takato–Ichinose area, Nagano Prefecture. Journal of Geological Society of Japan 90, 81–100 (in Japanese with English abstract).
Tullis, J., Christie, J.M., Griggs, D.T., 1973. Microstructures and preferred orientations of experimentally deformed quartzites. Geological Society of America Bulletin 84, 297–314.
Tullis, J., Yund, R.A., 1977. Experimental deformation of dry Westerly granite. Journal of Geophysical Research 82, 5705–5718.
Vauchez, A., 1980. Ribbon texture and deformation mechanisms of quartz in a mylonitized granite of Great Kabylia (Algeria). Tectonophysics 67, 1–12.
Vernon, R.H., Flood, P.H., 1988. Contrasting deformation of S- and I-type granitoids in the Lachlan Fold Belt, eastern Australia. Tectonophysics 147, 127–143.
Wenk, H.R., Pannetier, J., 1990. Texture development in deformed granodiorites from the Santa Rosa mylonite zone, southern California. Journal of Structural Geology 12, 177–184.
Wilson, C.J.L., 1973. The prograde microfabric in a deformed quartzite sequence, Mount Isa, Australia. Tectonophysics 19, 39–81.
Wilson, C.J.L., Bell, I.A., 1979. Deformation of biotite and muscovite: optical microstructure. Tectonophysics 58, 179–200.